

## **ANALYSIS OF CRYSTALLITE SIZE CHANGES IN A HEMATITE AND MAGNETITE FORMED ON STEEL USED IN THE POWER INDUSTRY**

***Monika Gwoździk***

Institute of Materials Engineering  
Faculty of Production Engineering and Materials Technology  
Częstochowa University of Technology

Received 27 July 2017, accepted 29 November 2017, available online 6 December 2017.

**K e y w o r d s:** 10CrMo9-10 steel, hematite, magnetite, X-ray diffraction, crystallite sizes.

### **A b s t r a c t**

The paper presents results of studies on the crystallite sizes of oxide layer formed during a long-term operation on 10CrMo9-10 steel at an elevated temperature ( $T = 545^\circ\text{C}$ ,  $t = 200,000 \text{ h}$ ). This value was determined by a method based on analysis of the diffraction line profile, according to a Scherrer formula. The oxide layer was studied on a surface and a cross-section at the outer and inner site on the pipe outlet, at the fire and counter-fire wall of the tube. X-ray studies were carried out on the surface of a tube, then the layer's surface was polished and the diffraction measurements repeated to reveal differences in the originated oxides layer.

## **Introduction**

Steels operating at elevated temperatures (such as e.g. 10CrMo9-10, 13CrMo4-5, X10CrMoVNb9-1) are exposed to a high-temperature corrosion, which frequently results in the damage of elements operating long-term in the power industry. The originating oxide layer grows with time and increasing temperature, which then results in a loss of tube wall thickness. Such thinning of the wall occurs both on the inside and on the outside. However, on the outside the corrosion is additionally supported by aggressive compounds

Correspondence: Monika Gwoździk, Instytut Inżynierii Materiałowej, Politechnika Częstochowska, ul. Armii Krajowej 19, 42-201 Częstochowa, e-mail: gwozdzik.monika@wip.pcz.pl

existing in the flue gas (GWOŹDZIK, NITKIEWICZ 2014, GWOŹDZIK 2016a,b). Numerous papers on the oxidation of steels used in the power industry were published in recent years. The papers refer both to the short-term (up to a few hundred hours) and to the long-term oxidation (up to a few thousand or even a few hundred thousand hours) (GWOŹDZIK, NITKIEWICZ 2014, GWOŹDZIK 2016a, GWOŹDZIK 2016b, SÁNCHEZ et al. 2009). A great interest in studies on steels operated during more than 100,000 hours results from forecasting the life of thermal-mechanical equipment planned to be operated for more than 300,000 hours (ŚLIWA, GAWRON, 2010, TRZESZCZYŃSKI 2011). Both short- and long-term studies show that the oxide layer formed on steels consists of a few layers. In paper (BISCHOFF et al. 2013) performed short-term studies on two steels, HCM12A and NF616. Corrosion test were performed in steam and SCW (super critical water) at 500°C. The paper showed, that both alloys in both corrosion environments formed of  $\text{Fe}_3\text{O}_4$  (outer layer) and a mixture of  $\text{Fe}_3\text{O}_4$  and  $\text{FeCr}_2\text{O}_4$  (inner layer). Also studies carried out by (CHEN et al. 2006) on steel NF16 and studies performed on steel X10CrMoVNb9-1 ( $T = 1,000$  h – SÁNCHEZ et al. 2009,  $T = 54,144$  h – GWOŹDZIK, NITKIEWICZ 2014) have shown a laminar structure of the oxide layer. At present the huge development in research equipment has taken place, especially using in materials engineering, such as: SEM, XRD, AFM, MFM, TEM (BRAMOWICZ et al. 2014, GWOŹDZIK 2016b, SZAFARSKA, IWASZKO 2012, LABISZ et al. 2016, 2017). Studies on oxidised layers are now carried out more and more often, with the application of XRD measurements. The study comprised a crystallite sizes of oxide layers formed on steels long-term operated at elevated temperatures.

## Material and Experimental Methods

The material studied comprised specimens of 10CrMo9-10 steel operated at the temperature of 545°C during 200,000 h. The chemical compositions and operating parameters of steel are given in Table 1. The analysis of the chemical composition of steel was carried out using spark emission spectroscopy on a Spectrolab spectrometer.

The oxide layer was studied at the outer site (the flowing gas side) and at the inner site (the flowing steam side) on the pipe outlet, at the fire and counter-fire wall of the tube.

X-ray diffraction (XRD) measurements (studying the phase composition, crystallite sizes); the layer was subject to measurements using a Seifert 3003T/T X-ray diffractometer and the radiation originating from a tube with a cobalt anode ( $\lambda_{\text{Co}} = 0.17902$  nm). X-ray studies were performed, comprising measurements in a symmetric Bragg-Brentano geometry. XRD measurements

Table 1  
Chemical composition of examined steel and parameters of exploitation

Chemical composition [wt. %]							
Acc.	C	Si	Mn	P	S	Cr	Mo
Analysis	0.11	0.34	0.55	0.002	0.009	2.23	0.98
EN	0.08–0.14	max. 0.50	0.40–0.80	max. 0.020	max. 0.010	2.00–2.50	0.90–1.10
Parameters of exploitation							
Temperature [°C]				time [h]			
545				200,000			

in the first stage (surface measurements and after the first polishing) were carried out in the range of 20÷120° angle for phase identification which were presented in paper (Gwoździk 2016b), then the measurements were narrowed to an angle range of 35÷45° with an angular step of 0.1° and exposure time 4 s. To interpret the results the diffractograms were described by a Pseudo Voigt curve using the Analyze software. A Pseudo Voigt function was used in order to accurately determine the location of the major diffraction reflections. A computer software and the PDF4+2009 crystallographic database were used for the phase identification.

Based on the width and the position of the main coat and substrate reflections, the size of the crystallites was determined using the Scherrer formula (1) (CULLITY 1964, Gwoździk 2016c):

$$D_{hkl} = \frac{k \cdot \lambda}{\beta \cdot \cos\theta} \quad (1)$$

where:

$D_{hkl}$  – crystallite size in the direction normal to  $(hkl)$  [nm],

k – constant (~1);

$\lambda$  – radiation wavelength [nm],

$\beta$  – reflection width depending on the crystallite size [rad],

$\theta$  – Bragg angle [rad].

X-ray studies were carried out on the surface, and then the layer surface was polished down and the diffraction measurements were performed again to determine individual oxide layers.

The size of the  $D_{hkl}$  crystallites size was determined for the reflections originating from the planes (104) for  $\text{Fe}_2\text{O}_3$  and (311) for  $\text{Fe}_3\text{O}_4$ , which are occurring at angles of 38.7464° and 40.8998°, respectively (according to the catalog card ICDD PDF 01-079-0007 and ICDD PDF 01-089-0951). The catalog standards for  $\text{Fe}_2\text{O}_3$  and  $\text{Fe}_3\text{O}_4$  have been shown on the Figure 1.

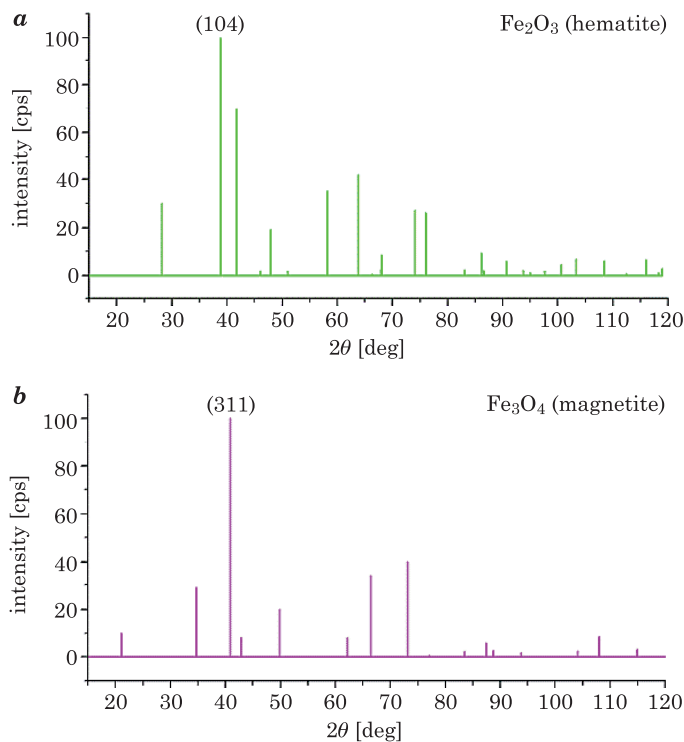


Fig. 1. Standards corresponding to individual oxides, in which the main reflections originating from planes are marked

X-ray measurements were performed at different depths of the oxide layer.

After removal of the sediment layer (400 µm, 10 µm, 6 µm and 4 µm, for outer site-fire wall, outer site-opposite fire wall, inner site-fire wall, inner site-opposite fire wall, respectively), X-ray measurements were carried out, then for each case, the oxide layer was removed (20 µm) cyclically, each time making XRD measurements:

- from exhaust side – fire side, the oxide layer was removed every 20 µm in 21 cycles,
- from exhaust side – counter-fire side, the oxide layer was removed every 20 µm in 18 cycles,
- from steam side – fire side, the oxide layer was removed every 20 µm in 21 cycles,
- from steam side – counter-fire side, the oxide layer was removed every 20 µm in 20 cycles.

The exemplary of examine of XRD measurements has been shown in Figure 2.

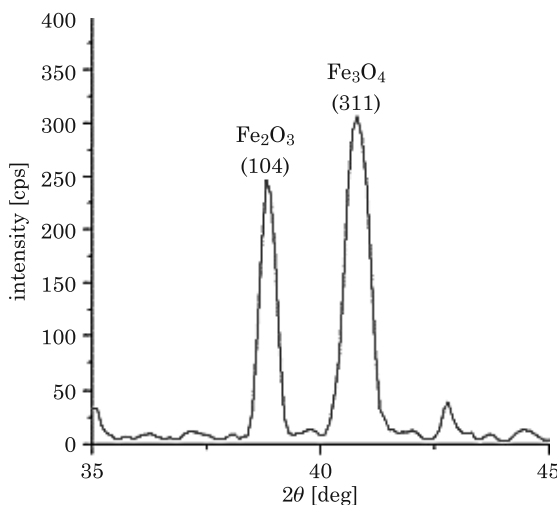


Fig. 2. X-ray diffraction patterns from the oxides layer obtained by means of XRD technique

## Results of examinations

The obtained results have shown that in the case of the fire side of the flue gas side after removing the correct the oxide layer by 20  $\mu\text{m}$ , the size of the  $D_{hkl}$  crystallites for hematite was the highest and it equals 49 nm (Fig. 3). Further successive removal of the hematite layer showed a decrease of crystallite size. For magnetite, the gradual increase was observed, the next delicate decrease and the next increase of crystallite sizes has been observed together with the

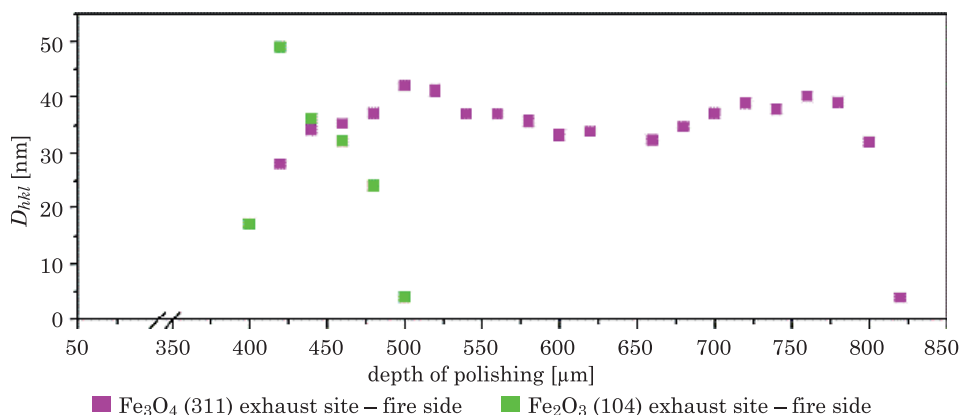


Fig. 3. Determination of crystallite size  $D_{hkl}$  for main peaks Fe<sub>3</sub>O<sub>4</sub> and Fe<sub>2</sub>O<sub>3</sub>, exhaust side – fire side

depth of polishing. The highest value of this parameter was obtained at a depth 500  $\mu\text{m}$  of oxide layer, where  $D_{hkl}$  was 42 nm.

In the case of the opposite-fire side of the flue gas side (Fig. 4), the  $D_{hkl}$  for hematite have been in the range of about 48 nm at a depth of 30  $\mu\text{m}$ . The sharp of decrease this parameter was observed at a depth of 50  $\mu\text{m}$ . In case of magnetite, the  $D_{hkl}$  is oscillated around 40 nm in a depth of oxide layer from 50 to 170  $\mu\text{m}$ . It has been shown decrease of crystallite size at a depth from 210  $\mu\text{m}$  to 230  $\mu\text{m}$  and increase of  $D_{hkl}$  in depth 250  $\mu\text{m}$ .

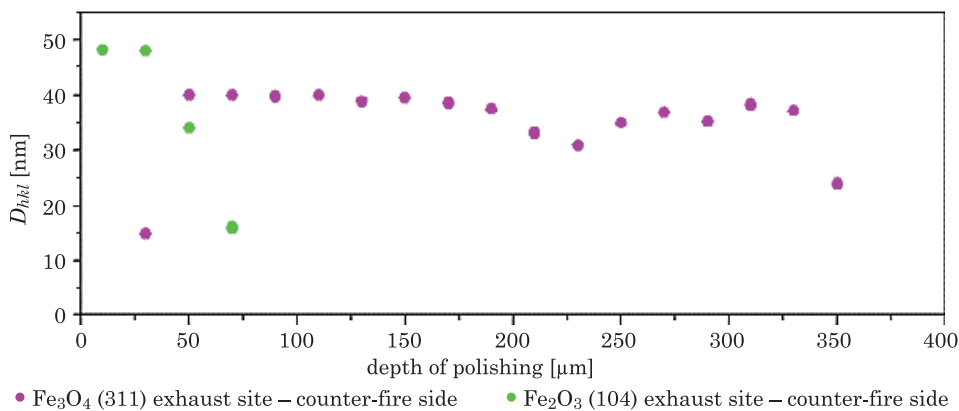


Fig. 4. Determination of crystallite size  $D_{hkl}$  for main peaks  $\text{Fe}_3\text{O}_4$  and  $\text{Fe}_2\text{O}_3$ , exhaust side – counter-fire side

The size of crystallites determined based on the Scherrer formula on the steam side shows smaller dimensions than from flue gas side. The parameter of  $D_{hkl}$  of hematite (for steam side) the largest values equal 46 nm and 44 nm for the fire side and the opposite fire side respectively (Fig. 5 and 6). In both cases, this parameter decreases dramatically in the depth of the layer is greater than 86  $\mu\text{m}$ . On the fire side, the polishing (up to 186  $\mu\text{m}$ ) has shown a delicate growth of crystallites of magnetite, the next series of polishing (from 186  $\mu\text{m}$  to 400  $\mu\text{m}$ ) has shown as small decrease of crystallite size. For the fire side, crystallite sizes of magnetite has been increasing up to a depth of 84  $\mu\text{m}$ . The next polishing (from 84  $\mu\text{m}$  to 164  $\mu\text{m}$ ) have shown that the crystallite size is maintained at one level. The polishing depth above 164  $\mu\text{m}$  has shown a decrease in  $D_{hkl}$  which oscillates around the same value up to a depth of polishing 380  $\mu\text{m}$ .

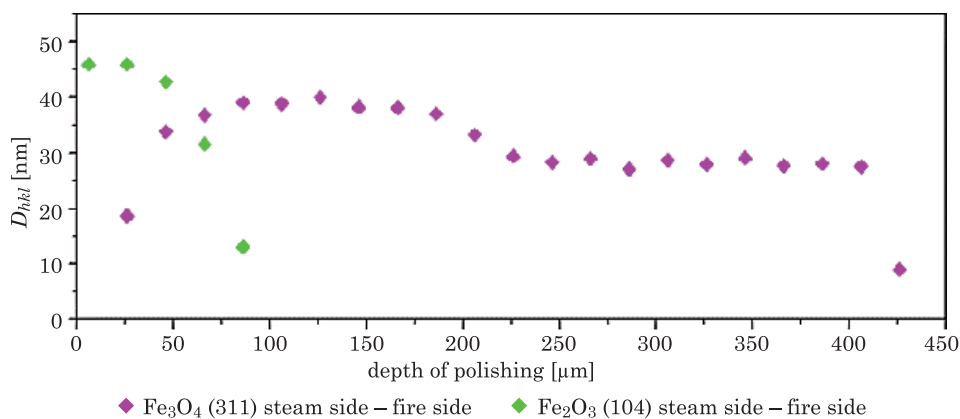


Fig. 5. Determination of crystallite size  $D_{hkl}$  for main peaks  $\text{Fe}_3\text{O}_4$  and  $\text{Fe}_2\text{O}_3$ , steam side – fire side

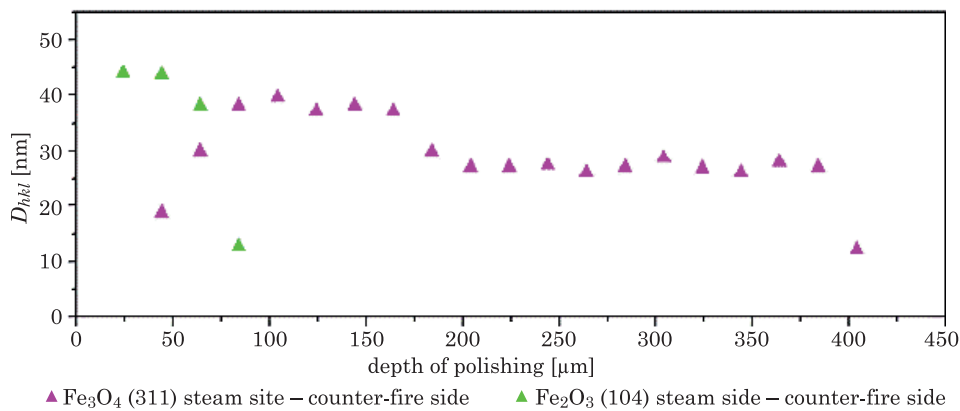


Fig. 6. Determination of crystallite size  $D_{hkl}$  for main peaks  $\text{Fe}_3\text{O}_4$  and  $\text{Fe}_2\text{O}_3$ , steam side – counter-fire side

## Summary

The paper presents results of studies on oxides formed on 10CrMo9-10 steel operated at the temperature of 545°C during 200,000 h. The oxide layer formed on the flue gas side (the outer side) and steam side (the inner side) both on the fire and counter-fire side were analyzed.

The investigated of oxide layer formed on this steel have shown more degraded of hematite and magnetite in the case of larger crystallites. The results obtained are well correlated with the results obtained with the use of an

optical microscope, as have shown in paper (GWOŹDZIK 2016b). The oxide layer thickness together with deposits on the fire side was 435 µm and 820 µm on the flowing medium and flue gas side, respectively. For the opposite fire side on the inside the oxides layer thickness was 405 µm while on the outside 360 µm. Examinations carried out have shown that the formed layer is the most degraded on the fire side from flue gas side. The size of crystallites on this side have been the largest dimensions both for hematite and magnetite. Instead, comparing the size of hematite and magnetite crystallites it is possible to state that in every cases  $D_{hkl}$  is larger for hematite. The size of crystallites in oxides originating during long-term operation depends on oxides morphology, where it has been presented in previous paper the author. In paper (GWOŹDZIK 2016c), the author showed that the size of crystallites determined based on the Scherrer formula on the fire side shows much larger dimensions for oxides. Instead, comparing the size of hematite and magnetite crystallites it is possible to state that  $D_{hkl}$  is larger for hematite.

## References

- BISCHOFF J., MOTTA A.T., EICHFELD C., COMSTOCK R.J., CAO G., ALLEN T.R. 2013. *Corrosion of ferritic-martensitic steels in steam and supercritical water*. Journal of Nuclear Materials, 441: 604–611.
- BRAMOWICZ M., KULESZA S., MROZEK G. 2014. *Changes in magnetic domain structure of maraging steel studied by magnetic force microscopy*. Technical Sciences, 17(4): 371–379.
- CHEN Y., SRIDHARAN K., ALLEN T.R., UKAI S. 2006. *Microstructural examination of oxide layers formed on an oxide dispersion strengthened ferritic steel exposed to supercritical water*. Journal of Nuclear Materials, 359: 50–58.
- CULLITY B.D. 1964. *Podstawy dyfrakcji promieni rentgenowskich*. PWN, Warszawa.
- EN 10028-2 *Flat products made of steels for pressure purposes. Part 2. Non-alloy and alloy steels with specified elevated temperature properties*.
- GWOŹDZIK M., NITKIEWICZ Z. 2014. *Studies on the adhesion of oxide layer formed on X10CrMoVNb9-1 steel*. Archives of Civil and Mechanical Engineering, 14: 335–341.
- GWOŹDZIK M. 2016a. *Structure studies of porous oxide layers formed on 13CrMo4-5 steels long-term operated in the power industry*. Technical Sciences, 19(3): 257–266.
- GWOŹDZIK M. 2016b. *The defects of oxide layers formed on 10CrMo9-10 steel operated for 200,000 hours at an elevated temperature*. Archives of Metallurgy and Materials, 2B(61): 987–992.
- GWOŹDZIK M. 2016c. *Analysis of Crystallite Size Changes in an Oxide Layer Formed on Steel Used in the Power Industry*. Acta Physica Polonica A, 4(130): 935–938.
- LABISZ K., KRUPIŃSKI M., PAWLĘTA M., MATUŚ K., KREMZER M., DOPIERALA K. 2016. *High Resolution TEM Investigations and TDA Analysis of Zinc Alloy with Strontium Addition*. Acta Physica Polonica A, 130(4): 823–826.
- LABISZ K., TAŃSKI T., KREMZER M., JANICKI D. 2017. *Effect of laser alloying on heat-treated light alloys*. International Journal of Materials Research, 108(2): 126–132.
- SZAFARSKA M., IWASZKO J. 2012. *Laser remelting treatment of plasma-sprayed Cr<sub>2</sub>O<sub>3</sub> oxide coatings*. Archives of Metallurgy and Materials, 57(1): 215–221.
- SÁNCHEZ L., HIERRO M.P., PÉREZ F.J. 2009. *Effect of chromium content on the oxidation behaviour of ferritic steels for applications in steam atmospheres at high temperatures*. Oxidation of Metals, 71: 173–186.

- ŚLIWA A., GAWRON P. 2010. *Wpływ warunków chemicznych pracy bloków energetycznych na możliwość przedłużania ich eksploatacji powyżej 300000 godzin.* XII Sympozjum Informacyjno-Szkoleniowe: „Diagnostyka i remonty urządzeń cieplno-mechanicznych elektrowni. Modernizacje urządzeń energetycznych w celu przedłużenia ich eksploatacji powyżej 300000 godzin”, Wisła, p. 23–28.
- TRZESZCZYŃSKI J. 2011. *System diagnostyczny zapewniający bezpieczną pracę bloków 200MW eksploatowanych powyżej 300000 godzin.* XIII Sympozjum Informacyjno-Szkoleniowe: „Diagnostyka i remonty urządzeń cieplno-mechanicznych elektrowni. Zarządzanie majątkiem produkcyjnym grupy elektrowni”, Katowice, p. 87–90.